International Journal of Thermophysics, Vol. 23, No. 1, January 2002 (© 2002)

Thermal Response of a Two-Phase Near-Critical Fluid in Low Gravity: Strong Gas Overheating as Due to a Particular Phase Distribution[1]

R. Wunenburger,[2,3] Y. Garrabos,[2] C. Lecoutre,[2] D. Beysens,[4] J. Hegseth,[5] F. Zhong,[6] and M. Barmatz[6]

An experimental study of the thermal response to a stepwise rise of the wall temperature of two-phase near-critical SF_6 in low gravity for an initial temperature ranging from 0.1 to 10.1 K from the critical temperature is described. The change in the vapor temperature with time considerably exceeds the change in the wall temperature (overheating by up to 23% of the wall temperature rise). This strong vapor overheating phenomenon results from the inhomogeneous adiabatic heating process occurring in the two-phase near-critical fluid while the vapor bubble is thermally isolated from the thermostated walls by the liquid. One-dimensional numerical simulations of heat transfer in near-critical two-phase ^{3}He confirm this explanation. The influence of heat and mass transfer between gas and liquid occurring at short time scales on the thermal behavior is analyzed. A model for adiabatic heat transfer, which neglects phase change but accounts for the difference between the thermophysical properties of the vapor and those of the liquid, is presented. A new characteristic time scale of adiabatic heat transfer is derived, which is found to be larger than that in a one-phase liquid and vapor.

KEY WORDS: adiabatic compression; low gravity; near-critical fluid; two-phase heat and mass transfer.

[1] Paper presented at the Fourteenth Symposium on Thermophysical Properties, June 25–30, 2000, Boulder, Colorado, U.S.A.

[2] Equipe du Supercritique pour l'Environnement, les Matériaux et l'Espace, Institut de Chimie de la Matière Condensée de Bordeaux UPR CNRS 9048, Université Bordeaux I, Avenue du Dr. A. Schweitzer, F-33608 Pessac Cedex, France.

[3] To whom correspondence should be addressed. E-mail: wunenbur@lps.ens.fr

[4] Equipe du Supercritique pour l'Environnement, les Matériaux et l'Espace, Service des Basses Températures, Commissariat à l'Energie Atomique, 17 rue des Martyrs, F-38054 Grenoble Cedex 9, France.

[5] Department of Physics, University of New Orleans, New Orleans, Louisiana 70148, U.S.A.

[6] Jet Propulsion Laboratory, California Institute of Technology, 4800 Oak Grove Drive, Pasadena, California 91109-8099, U.S.A.

0195-928X/02/0100-0103/0 © 2002 Plenum Publishing Corporation

1. INTRODUCTION

As the liquid–vapor critical point (CP) is approached, many thermodynamic and transport properties of pure fluids exhibit striking behavior [1]. Notable examples include the divergence in the isothermal compressibility and the vanishing thermal diffusivity. In fluids confined in a constant volume, heat may be transferred by both thermal diffusion and adiabatic compression. This adiabatic compression is called "the piston effect" because an expanding hot boundary layer acts as a piston to compress the interior of the fluid, increasing its temperature [2–6]. In pure fluids heat diffusion is slower, whereas the piston effect is faster, as the CP is approached. The latter process becomes dominant in near-critical fluids, leading to very fast thermalization. The adiabatic nature of the fast thermal equilibration in supercritical homogeneous fluid samples is now well established, after being confirmed by numerous experiments performed on the ground [7, 8] and in weightlessness [9–12], where convection is absent.

The thermal equilibration of near-critical stratified one-phase or two-phase fluids is more complicated to characterize. As first theoretically predicted by Onuki and Ferrell [5], then numerically and experimentally observed in stratified one-phase fluids [7, 13] and two-phase fluids [8, 14, 15], the inhomogeneity of the thermodynamic properties of the fluid leads to an inhomogeneous temperature response inside the sample; i.e., the adiabatic heating induces temperature gradients within the sample. A striking consequence of adiabatic heat transfer in stratified fluids is the occurrence of an overshoot of the temperature in the region of lower density beyond the temperature of the thermostat when a positive temperature step change (initial temperature T_i, final temperature $T_f > T_i$) is imposed by the thermostat. This phenomenon was first observed in a two-phase fluid during an experiment dedicated to the study of near-critical "boiling" [16]. A more detailed study was performed [17] in pure SF_6 using the Alice 2 facility onboard the MIR station during the French–Russian Perseus mission (February–August 1999), as part of the French–American GMSF scientific program. This transient phenomenon would be unthinkable for purely diffusive, isobaric equilibration processes, since it would violate the second law of thermodynamics. On the other hand, when the volume of the fluid sample is constant, this phenomenon is possible even at large distances from the CP. Indeed the temperature change in the fluid is due not only to heat diffusion but also to adiabatic compression, i.e., to the work done by pressure changes that are subjected to mechanical equilibrium conditions and not to thermal equilibrium conditions.

In Section 2 we briefly present experimental observations of the vapor overheating phenomenon. In Section 3 we investigate the influence of the

distribution of the phases inside the cell on the magnitude of the gas overheating phenomenon by means of a one-dimensional numerical model developed by one of us [8] and explain why such a large vapor overheating could be measured in low gravity. In Section 4, we present a simple analytical model of the characteristic time of the piston effect t_{PE} in two-phase near-critical fluids, valid when vapor is not in contact with the walls of the thermostat. This model accounts for the difference between the thermophysical properties of liquid and those of vapor, and results in an expression for t_{PE} slightly different from its usual form established for homogeneous one-phase near-critical fluids by Onuki et al. [2].

2. EXPERIMENTAL INVESTIGATION OF TWO-PHASE HEAT TRANSFER

2.1. Experimental Apparatus

The Alice 2 facility, whose detailed description is given in Ref. 18, integrates a management system for diagnostics and stimuli with a regulation system that controls the temperature of a sample cell to within a few tens of microkelvins. The experimental cell used for this study was made of a CuCoBe alloy. The internal fluid volume was a cylinder (12-mm internal diameter, 6.7-mm thickness) sandwiched between two parallel sapphire windows. The inner surface of one of the sapphire windows was coated with a dielectric that forms an interferometric mirror. A Yellow Spring Instrument Co. 44900 thermistor (2-s rise time, 100-μK accuracy) imbedded in the sample cell unit near the fluid volume was used to follow the temperature evolution of the cell walls (labeled T_W).

The cell was filled with pure SF_6 at its critical density ($\pm 0.1\%$). The initial two-phase distribution in low gravity consisted of a gas bubble surrounded by the liquid that wetted the walls of the cell, whose interferometric image is shown in Fig. 1a. The bubble touched the sapphire windows, and its cross section is shown schematically in Fig. 1b. Three Thermometrics B10 thermistors (10-ms rise time, 500-μK accuracy, 0.2-mm diameter) were placed in the cell volume, allowing local measurements of the fluid temperature. Two of them (labeled Th1 and Th2) were located close to the cell wall (roughly 1 mm) and were always observed to be in the liquid. The temperatures measured by Th1 and Th2 are labeled T_L^1 and T_L^2. The third thermistor (Th3) was mounted in the center of the cell, so that in the usual low gravity environment of the Mir station (residual acceleration of the order of $10^{-4}g$, where g is the acceleration of Earth's gravity), the gas bubble, of volume fraction 0.5, was always found to contain thermistor Th3 (see Fig. 1a). The temperature measured by Th3 is labeled T_V. The

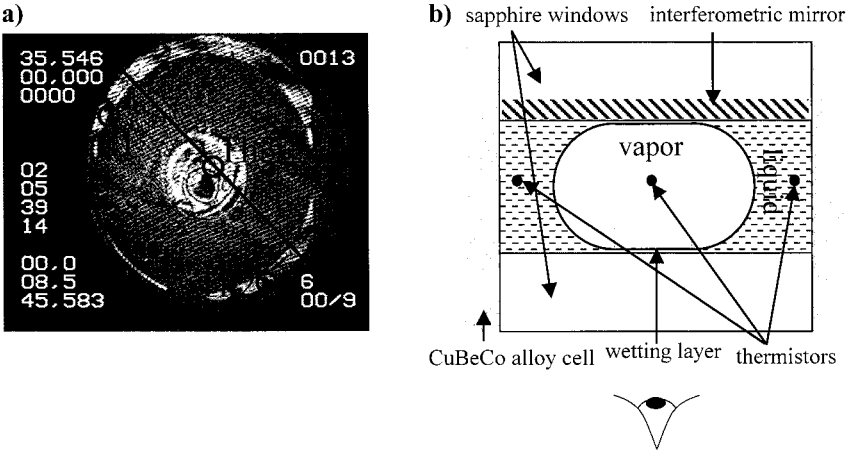

Fig. 1. (a) Image of the interferometric cell during a +100 mK quench ($T_i = T_c - 10.1$ K) looking through the cell window. Circles: positions of thermistors, labeled Th1, Th2, and Th3. Solid line: thermistor thread. (b) Schematic cross section of the experimental cell.

measuring frequencies were 25 Hz for T_L^1, T_L^2, and T_V and 1 Hz for T_W during the first 5 min following the quench, then 0.1 Hz during the next 55 min. The image of the sample obtained through the Twyman–Green interferometer was recorded by a CCD camera at a frequency of 25 Hz.

2.2. Observation of the Gas Overheating Phenomenon

The properties of the vapor and the liquid phases vary according to universal power laws with the critical temperature difference, $T_c - T$ [1] (T is the temperature, T_c is the liquid–vapor critical temperature). We performed the heat transfer experiments relatively far from the CP so that we could take advantage of the large thermophysical differences between the gas and the liquid to magnify the difference between the adiabatic responses of each phase.

A series of positive wall step changes in temperature were performed with $\Delta T = T_f - T_i = 100$ and 50 mK for T_i ranging from $T_c - 10.1$ K to $T_c - 0.1$ K. A wall temperature rise of amplitude ΔT consisted of a sharp linear increase in T_W up to 80% of ΔT in less than 10 s, followed by a smooth evolution up to the final temperature T_f. As an example, the evolution of T_W, T_L^1, T_L^2, and T_V during a T_W rise of $\Delta T = +100$ mK from $T_i = T_c - 10.1$ K is shown in Fig. 2. During each rise of T_W the temperatures measured in the liquid, T_L^1 and T_L^2 always remained lower than T_W. On the other hand, before the end of each rise of T_W, T_V passed well beyond T_L^1

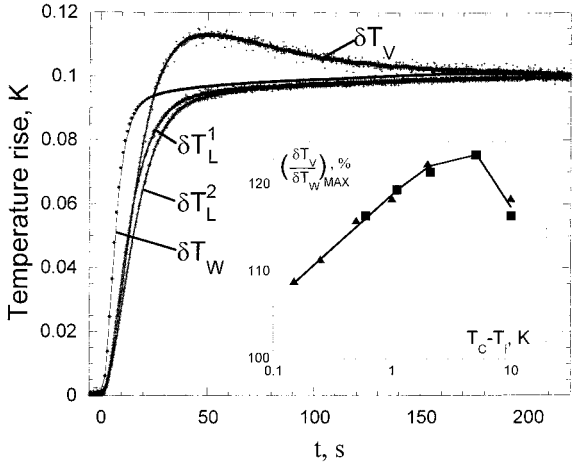

Fig. 2. Temperature rise at the cell wall, δT_W, in the liquid, δT_L^1 and δT_L^2, and in the vapor, δT_V ($\delta T_X = T_X - T_i$, i = L, V, W), during a wall temperature rise of amplitude $\Delta T = 100$ mK from $T_i = T_c - 10.1$ K. Inset: Maximum reduced vapor overheating $(\delta T_V/\delta T_W)_{MAX}$, expressed in percentage, as a function of $T_c - T_i$. Squares: $\Delta T = 100$ mK. Triangles: $\Delta T = 50$ mK. Solid lines are a guide for the eye.

and T_L^2 and, more strikingly, also well beyond T_W. To compare the gas overheating detected during rises of T_W of different amplitudes, the temperature rise in the gas δT_V was scaled to the temperature rise of the cell walls δT_W (the rise of any temperature T_X is defined as $\delta T_X = T_X - T_i$), and the behavior of its maximum $(\delta T_V/\delta T_W)_{MAX}$ as a function of $T_c - T_i$ is plotted in the inset in Fig. 2. It exhibits a maximum of 123% around $T_c - T_i \approx 5$–7 K.

The vanishing differences in thermophysical properties between gas and liquid at the CP imply that, asymptotically near the CP, vapor and liquid show the same thermal response. On the other hand, far from the CP, the efficiency of the adiabatic heating is reduced and the heat transfer is mainly diffusive, a situation that prevents the gas overheating. The existence of a maximum for the gas overheating at $T < T_c$ is then due to the competition between an increasing efficiency of the adiabatic heating process and a decreasing difference of behavior between gas and liquid as the CP is approached.

3. INFLUENCE OF THE PHASE DISTRIBUTION ON OVERHEATING

We propose a qualitative explanation of the gas overheating phenomenon and discuss the influence of the phase distribution inside the experimental

cell on the magnitude of the vapor overheating using the results of one-dimensional (1-D) numerical simulations.

3.1. Qualitative Explanation

During the adiabatic heat transfer process, the pressure increase due to the expansion of the fluid heated at the boundary can be considered as homogeneous within the sample on time scales much longer than the time of flight of sound waves.

During the short period of efficiency of the piston effect, neither heat nor mass can be transferred between vapor and liquid initially at coexistence because of the weak thermal diffusivity near the CP. Onuki and Ferrell [5] pointed out that during the period of efficiency of the adiabatic heating, liquid and vapor should behave as if they were monophasic and that the temperature increase in the liquid δT_L and vapor δT_V should be isentropic such that

$$\frac{\delta T_V}{\delta T_L} = \frac{(\partial T/\partial P)_S^V}{(\partial T/\partial P)_S^L} \tag{1}$$

Since $(\partial T/\partial P)_S^V > (\partial T/\partial P)_S^L$, the vapor should be more rapidly heated than the liquid. This argument explains why the vapor temperature can exceed the liquid temperature. It is the phase distribution that permits the vapor temperature to exceed the cell wall temperature, as discussed below.

In a low-gravity environment, due to the perfect wetting of the liquid on the solid walls, the vapor forms a bubble that can be almost completely isolated from the thermostated cell walls by the liquid if particular geometrical conditions are satisfied (cell volume close enough to the spherical geometry, no perturbing effect of the sensors [15, 17]). This phase distribution is schematically shown in 1-D in Fig. 3b. On Earth, the buoyancy forces cause the liquid to be on the bottom of the cell, the vapor to be on the top, and both to be in contact with the cell walls (if we neglect the thin liquid wetting layers). This phase distribution is schematically shown in 1-D in Fig. 3a. During a temperature rise, the adiabatic heating process stops when the temperature gradient at the wall vanishes. If every cell wall is thermostated (as in Fig. 3a), under Earth's gravity two kinds of hot boundary layers (HBL) develop at the boundaries, one in the vapor and one in the liquid. We define the bulk liquid (bulk vapor) as the region between the liquid (vapor) HBL at the cell wall and the boundary layer developing at the gas–liquid interface, which is heated only by adiabatic compression. In both phases the HBL stops its expansion when the bulk temperature reaches T_W. When T_V^{bulk} exceeds T_W, the vapor HBL may even

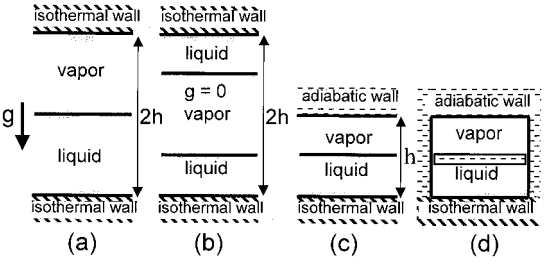

Fig. 3. 1-D sketch of the phase distribution of liquid and vapor (a) under Earth's gravity and (b) in low gravity. Gray: thermal boundary layers. Arrows show the direction of heat transfer and the direction of expansion of the HBL. (c) 1-D cell and phase distribution equivalent to b. (d) Three-domain model of the adiabatic heat transfer presented in Section 4. The liquid–vapor interface is replaced by an adiabatic, freely moving piston preventing heat and mass exchange between liquid and vapor.

contract (cooling piston effect) if the liquid HBL continues to expand to compensate for vapor overheating. In this simplified description, the piston effect cannot generate any overheating.

This scenario is noticeably different from what happens when only liquid is in contact with the thermostated cell walls (Fig. 3b), a situation that prevails in the experiment reported in Section 2 (the contact area between the vapor bubble and the sapphire windows is less than 6% of the overall heating area). In this case the adiabatic heating process stops when T_L^{bulk} has reached T_W. Before the equilibration of T_L^{bulk} and T_W, the bulk vapor (as defined as the homogeneous interior of the bubble, excluding any boundary layer) is heated more than the bulk liquid by the homogeneous pressure increase. Since the vapor bubble is not in contact with the heating wall, its temperature has no influence on the temperature gradient that drives the expansion of the liquid HBL. T_V^{bulk} can thus exhibit a large overshoot, as confirmed by the measurements obtained by thermistor Th3, located in the middle of the vapor bubble.

3.2. Numerical 1-D Study of the Effect of the Phase Distribution on the Vapor Overheating

To check the validity of the above qualitative explanation, we performed 1-D numerical simulations of the heat transfer in the near-critical region in two-phase ^{3}He. This numerical simulation is presented in detail in Ref. 8, where it was used to study the adiabatic heat transfer for a phase

distribution encountered under Earth's gravity, shown schematically in Fig. 3a. The thermophysical properties of ^{3}He were computed using the restricted cubic model of the equation of state whose parameters are given in Refs. 7 and 19. The similarity between the thermal responses of simulated ^{3}He and SF_6 to a rise in the wall temperature are guaranteed by the universal thermodynamic behavior of pure fluids near their critical point.

In the 1-D simulation, the phase distribution encountered in low gravity is accounted for by replacing the thermostated wall in contact with the vapor (Fig. 3a) with an isolated wall (Fig. 3c); i.e., we replaced the isothermal condition $T\ (x=0, t)=T_f$ at the upper wall (Fig. 3a) with the adiabatic condition $\partial T/\partial x(x=0, t)=0$ (Fig. 3c). For symmetry reasons, the resulting 1-D heat transfer problem in the cell shown schematically in Fig. 3c is fully equivalent to the 1-D problem, illustrated in Fig. 3b, of a vapor layer sandwiched between two liquid layers of equal thickness in contact with the two isothermal walls of a 1-D cell two times higher than the cell in Fig. 3c. The phase distribution in Fig. 3c deals with one liquid–vapor interface only and is the best 1-D representation of the 3-D phase distribution in low gravity as encountered in the experiment presented in Section 2.

The numerical simulations presented in the following were performed by imposing an ideal temperature step at the wall in contact with the liquid. The maximum of the vapor temperature was obtained at the adiabatic cell wall. In Fig. 4, we plot the maximum of the temperature increase in ^{3}He vapor obtained in the simulation scaled by the amplitude of the wall temperature rise $(\delta T_V/\Delta T_W)_{MAX}-1$ (expressed in %) as a function of the reduced critical temperature distance $\varepsilon=(T_c-T_i)/T_c$. These numerical results reproduce qualitatively well the strong vapor overheating phenomenon measured in SF_6, also shown in Fig. 4.

As shown in Fig. 4, at the initial reduced temperature of $\varepsilon=10^{-2}$ the calculated $(\delta T_V/\Delta T_W)_{MAX}-1$ (from Ref. 15) for ^{3}He in the phase distribution of Fig. 3a is smaller than that in the phase distribution of Fig. 3c. This shows the influence of the phase distribution on the magnitude of the vapor overheating.

3.3. Effect of the Liquid–Vapor Transition on the Vapor Overheating

During the temperature increase in liquid and vapor due to the adiabatic heat transfer process, only a thin layer of fluid is able to remain at liquid–vapor coexistence, and the temperature difference between the vapor bulk and the liquid bulk causes heat and mass flow through the interface so as to equilibrate the chemical potential near the interface [5]. The entropy

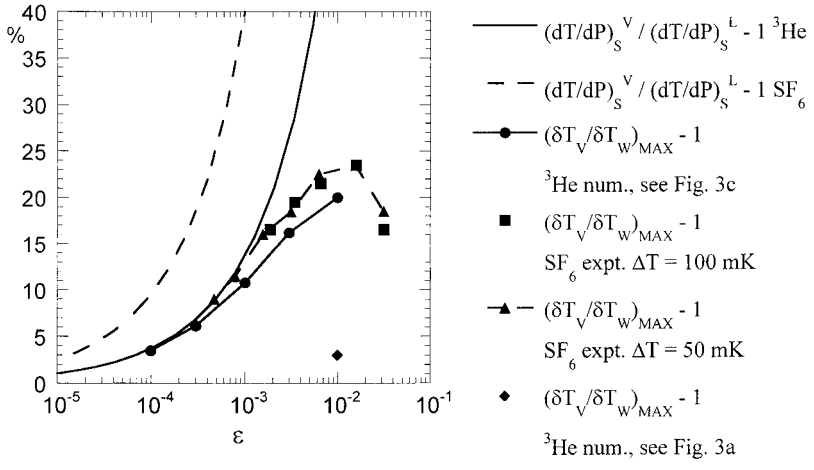

Fig. 4. Comparison between vapor overheating and prediction of Eq. (1). Circles (solid lines as a guide for the eye): maximum reduced ^{3}He vapor overheating, $(\delta T_V/\Delta T_W)-1$, computed numerically as a function of $\varepsilon=(T_c-T_i)/T_c$ with the vapor isolated from the thermostated cell wall (Fig. 3b). Diamond: maximum reduced vapor overheating computed with the vapor in contact with the thermostated cell wall reported in Ref. 8 (Fig. 3a). Solid line: $[(\partial T/\partial P)_S^V/(\partial T/\partial P)_S^L]-1$ computed for ^{3}He using the restricted cubic model of the equation of state (EOS). Squares and triangles (dashed lines as a guide for the eye): maximum reduced vapor overheating, $(\delta T_V/\Delta T_W)-1$, determined experimentally in SF_6 as a function of ε. Dashed line: $[(\partial T/\partial P)_S^V/(\partial T/\partial P)_S^L]-1$ computed for SF_6 using the EOS of Ref. 21.

conservation at the interface implies [20] $dm_{vap}/dt=(\lambda_V\nabla T_V-\lambda_L\nabla T_L)/\Delta h$, where dm_{vap}/dt is the rate of vaporization of liquid, Δh is the latent heat of vaporization, and $\lambda_V\nabla T_V-\lambda_L\nabla T_L$ is the heat transported to the interface, which is negative at the beginning of the adiabatic heating. Hence, the adiabatic heating process causes condensation of vapor at the interface at the beginning of the temperature rise. This condensation was numerically observed by Zhong and Meyer [8]. Condensation reduces the mass of vapor and is equivalent to a weaker compression, whereas it increases the mass of liquid and is equivalent to a larger compression. Due to condensation, vapor is less heated and liquid is more heated, leading to a vapor overheating smaller than the one deduced from the prediction of Onuki and Ferrell [5] [Eq. (1)]. In Fig. 4, the vapor maximum overheating measured in SF_6 is compared to the ideal overheating without any phase change at the interface $[(\partial T/\partial P)_S^V/(\partial T/\partial P)_S^L]-1$ [computed using the equation of state (EOS) of Ref. 21]. The difference between them demonstrates the weakening effect on the vapor overheating of the phase change at the interface during the temperature change.

The magnitude of the mass transfer at the interface occurring during the adiabatic heat transfer process should depend mainly on the value of t_{PE}, the interface area, the heating surface area, and the sharpness of the wall temperature rise (characteristic time of the temperature increase of the walls). The comparison between the reduced ^{3}He vapor maximum overheating $(\delta T_V/\Delta T_W)_{MAX}-1$ and the values of $[(\partial T/\partial P)_S^V/(\partial T/\partial P)_S^L]-1$ in Fig. 4 indicates that, even when the wall temperature rise is stepwise, the phase change at the interface significantly weakens the vapor overheating when $\varepsilon > 3\times 10^{-4}$. A detailed numerical investigation of the causes of the weakening of the vapor overheating is presently in progress.

4. MODEL OF THE CHARACTERISTIC TIME OF THE PISTON EFFECT IN A TWO-PHASE FLUID

The EOS of Ref. 21 shows that the most rapidly divergent ratios of the thermophysical properties of liquid and vapor are $(\partial T/\partial P)_\rho^L/(\partial T/\partial P)_\rho^V$ and $(\partial \rho/\partial P)_T^V/(\partial \rho/\partial P)_T^L$. Thus, the correction of t_{PE} proposed by Onuki and Ferrell [5] for the case of an inhomogeneous one-phase fluid, $t_{PE} = L^2/[D_T^{BL}(C_P^{BL}/\langle C_V\rangle)^2]$ (where BL labels the property of the fluid in the boundary layer, and $\langle C_V\rangle$ is the average over the sample of C_V), should not be adapted to two-phase fluids, since it is based on the assumption of homogeneity of $(\partial T/\partial P)_S$ throughout the fluid sample. To take into account the differences between all the thermophysical properties of liquid and vapor, we propose a simple model of adiabatic heat transfer in two-phase fluids, where heat and mass transfer between the two phases are neglected during the period of efficiency of the adiabatic heat transfer. This is equivalent to assuming an adiabatic, freely moving piston in place of the fluid interface, as shown schematically in Fig. 3d, and both phases, initially at coexistence, evolve as one-phase fluids during the temperature rise. The assumed phase distribution is the one encountered in low gravity, without contact between vapor and the thermostated cell walls.

The same type of thermodynamic transformation as performed by Onuki et al. [2] leads to the following equation of evolution of the temperature in the bulk liquid T_L^{bulk}:

$$\frac{\partial T_L^{bulk}}{\partial t} = (\gamma^L - 1)\frac{\dot{Q}}{\rho^L C_V^L \Omega}\left(1+\Phi^V\left(\frac{\kappa_S^V}{\kappa_S^L}-1\right)\right)^{-1} \tag{2}$$

where γ is the usual ratio of the specific heats, $\dot{Q}$ is the rate of heat injected into the liquid HBL, Ω is the volume of the sample, Φ^V is the vapor volume fraction, and $\kappa_S = \rho^{-1}(\partial\rho/\partial P)_S$. $H = 1+\Phi^V((\kappa_S^V/\kappa_S^L)-1)$ accounts for the

mean compressibility of the two-phase fluid, which is larger than the compressibility of the liquid. Assuming a pure diffusive temperature profile in the liquid HBL as in Ref. 2, the time derivative of the total heat injected into the HBL reads $\dot{Q} = \lambda_L A(T_W - T_L^{bulk})/(\pi D_T^L t)$, where A is the surface of the heating wall and D_T^L is the thermal diffusivity of the liquid. The characteristic time scale associated with the piston effect, which is the time needed for T_L^{bulk} to reach T_W, is equal to $t_{PE} = \pi L^2/[D_T^L(\gamma - 1)^2]$ for a one-phase homogeneous near-critical liquid [2] corrected by the factor H^2:

$$t_{PE} = \frac{\pi L^2}{D_T^L(\gamma^L - 1)^2} H^2 \tag{3}$$

where $L = \Omega/A$. $H > 1$, implying that the piston effect characteristic time scale is larger for a two-phase fluid than for a one-phase liquid at the same temperature. The reason for this difference is the larger compressibility of vapor compared to liquid (this property is also responsible for the decrease in the sound speed in two-phase fluids). In Fig. 5 the variation of t_{PE} as a function of $T_c - T$ is shown for a one-phase liquid, a one-phase vapor, and a two-phase fluid with $L = 1$ mm. Also shown is the characteristic time scale of isobaric thermal diffusion L^2/D_T, computed with $L = 1$ mm for

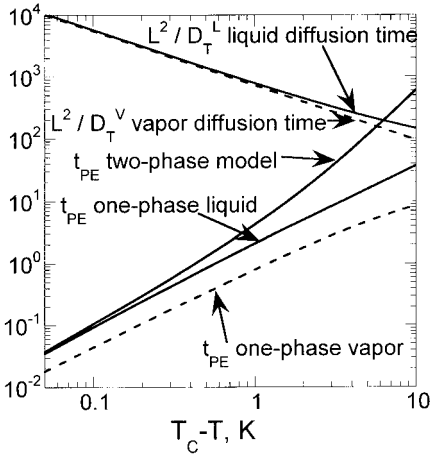

Fig. 5. The different characteristic time scales, expressed in seconds, of the piston effect t_{PE} and isobaric thermal diffusion L^2/D_T, computed for a characteristic length scale, $L = 1$ mm, for SF_6 using the EOS of Ref. 21 and the values of D_T given in Ref. 22, as a function of $T_c - T$.

SF_6 using the EOS of Ref. 21 and the values of D_T given in Ref. 22. Note that the difference between t_{PE} for a one-phase liquid and t_{PE} for this model is found to be significant for $T_c - T > 1$ K.

5. CONCLUSION

As shown experimentally, the adiabatic heat transfer in near-critical two-phase fluids can lead to the paradoxical overheating of vapor. Our 1-D numerical simulations show that the qualitative explanation presented in Section 3.1 of the influence of the phase distribution on the magnitude of the vapor overheating is relevant. Numerical investigation of the effect of phase change on the magnitude of the vapor overheating is in progress. The model for the characteristic piston effect time scale in two-phase fluids presented in Section 4 takes into account the difference in thermophysical properties between liquid and vapor. A further improvement of this model would be to include the effect of phase change on t_{PE}. Moreover, the validity of this model should be tested experimentally.

ACKNOWLEDGMENTS

This work was supported by CNES. The authors thank the team of the Perseus mission and the MIR station crew for their technical support, especially J. F. Zwilling and the French cosmonaut J. P. Haigneré. J.H., F.Z., and M.B. gratefully acknowledge the support of NASA.

REFERENCES

1. H. E. Stanley, *Introduction to Phase Transitions and Critical Phenomena* (Oxford, Clarendon Press, 1971).
2. A. Onuki, H. Hao, and R. A. Ferrell, *Phys. Rev. A* **41**:2256 (1990).
3. H. Boukari, J. N. Shaumeyer, M. E. Briggs, and R. W. Gammon, *Phys. Rev. A* **41**:2260 (1990).
4. B. Zappoli, D. Bailly, Y. Garrabos, B. Le Neindre, P. Guenoun, and D. Beysens, *Phys. Rev. A* **41**:2264 (1990).
5. A. Onuki and R. A. Ferrell, *Physica A* **164**:245 (1990).
6. B. Zappoli and P. Carlès, *Eur. J. Mech. B* **14**:41 (1995).
7. F. Zhong and H. Meyer, *Phys. Rev. E* **51:** 3223 (1995).
8. F. Zhong and H. Meyer, *Phys. Rev. E* **53**:5935 (1996).
9. J. Straub, A. Haupt, and L. Eicher, *Phys. Rev. E* **51**:5556 (1995).
10. R. de Bruijn, R. J. J. van Diest, T. D. Karapatsios, A. C. Michels, W. A. Wakeham, and J. P. M. Trusler, *Physica (Amsterdam)* **242A**:119 (1997).
11. T. Fröhlich, P. Guenoun, M. Bonetti, F. Perrot, D. Beysens, Y. Garrabos, B. Le Neindre, and P. Bravais, *Phys. Rev. E* **52**:1544 (1996).
12. Y. Garrabos, M. Bonetti, D. Beysens, F. Perrot, T. Fröhlich, P. Carlès, and B. Zappoli, *Phys. Rev. E* **57**:5665 (1998).

13. H. Boukari, R. L. Pego, and R. W. Gammon, *Phys. Rev. E* **52**:1614 (1995).
14. J. Straub and L. Eicher, *Phys. Rev. Lett.* **75**:1554 (1995).
15. L. Eicher, Ph.D. thesis (Münich, Germany, 1996).
16. Y. Garrabos, C. Chabot, R. Wunenburger, J. P. Delville, and D. Beysens, *J. Chim. Phys.* **96**:1066 (1999).
17. R. Wunenburger, Y. Garrabos, C. Lecoutre-Chabot, D. Beysens, and J. Hegseth, *Phys. Rev. Lett.* **84**:1400 (2000).
18. R. Marcout, J. F. Zwilling, J. M. Laherrere, Y. Garrabos, and D. Beysens, *Micrograv. Q* **5**:162 (1995).
19. F. Zhong and H. Meyer, *J. Low Temp. Phys.* **114**:231 (1999).
20. A. Onuki, *Phys. Rev. A* **43**:6740 (1991).
21. A. K. Wyczalkowska and J. V. Sengers, *J. Chem. Phys.* **111**:1551 (1999).
22. P. Jany and J. Straub, *Int. J. Thermophys.* **8**:165 (1987).